

- [13] a) M. Freund, L. Bodalbhai, A. Brajter-Toth, *Talanta* **1991**, *38*, 95. b) T. Osaka, T. Fukuda, H. Kanagawa, T. Momma, S. Yamauchi, *Sens. Actuators B* **1993**, *13*, 205. c) A. Ersöz, V. G. Gavalas, L. G. Bachas, *Anal. Bioanal. Chem.* **2002**, *372*, 786.
- [14] a) T. Cassagneau, T. E. Mallouk, J. H. Fendler, *J. Am. Chem. Soc.* **1998**, *120*, 7848. b) B. Bergman, T. W. Hanks, *Macromolecules* **2000**, *33*, 8035.
- [15] G. Gustafsson, L. Lundström, B. Lieberg, C. R. Wu, O. Inganäs, O. Wennerström, *Synth. Met.* **1989**, *31*, 163.
- [16] T. Cassagneau, F. Caruso, *Adv. Mater.* **2002**, *14*, 1629.

ZnO Nanoneedles Grown Vertically on Si Substrates by Non-Catalytic Vapor-Phase Epitaxy**

By Won Il Park, Gyu-Chul Yi,* Miyoung Kim, and Stephen J. Pennycook

There has been considerable interest in the growth of one-dimensional (1D) semiconductor nanostructures including nanowires.^[1–3] In addition to nanowires, semiconductor nanoneedles are of particular interest because their tips show a sharp curvature, offering potential applications as probing tips with high spatial resolution in both vertical and horizontal dimensions or field-emission tips due to the increased field-enhancement factor.^[4,5] Nevertheless, semiconductor nanoneedles have rarely been studied, while numerous semiconductor nanowires including Si, InP, GaN, GaAs, GaP, and ZnO have been synthesized.^[1–3,6] To prepare the nanowires, metal-catalysis-assisted vapor-liquid-solid (VLS) deposition has been widely employed because this method was used for Si micro-whisker growth in the 1960s.^[7] Since as-grown nanowires prepared by the VLS method yield a metal nanoparticle on their tips, nanoneedles with sharp tips are difficult to prepare using the VLS method. However, we recently developed a metal-catalyst-free growth method for preparing 1D nanostructures,^[8] which enables the growth of sharp-tipped ZnO nanoneedles.

One-dimensional ZnO nanowires and nanorods have been studied recently for optoelectronic nanodevice applications as the material has a wide and direct fundamental bandgap energy of 3.4 eV, a large excitonic binding energy of ~60 meV, and high mechanical and thermal stabilities.^[9] Both ZnO films and nanostructures have been prepared, typically on sapphire substrates as the substrate shows a good lattice match with ZnO.^[10–12] Nevertheless, the use of Si substrates enables the deposition of nanomaterials on large and cheap substrates,

offering possible mass production of the nanomaterials. More importantly, the preparation of nanomaterials on Si represents a breakthrough for nanomaterial integration in Si-based electronic devices. Despite the importance of the nanomaterials growth on Si substrates, vertically well-aligned one-dimensional ZnO nanostructure growth on Si has rarely been reported.^[6,13] Here, we report metal-organic chemical vapor deposition (MOCVD) of vertically well-aligned ZnO nanoneedles on Si substrates and their structural and optical characteristics.

The surface morphology of as-grown ZnO nanoneedles on Si substrates was investigated using scanning electron microscopy (SEM). As shown in Figures 1a–1c, a high density of ZnO nanoneedles is vertically aligned over the entire substrate and they exhibit sharp tips. The diameter and aspect ratio of ZnO nanoneedles depend on growth conditions including growth time. Typically, nanoneedles grown for 1 h exhibit mean lengths of 740 ± 50 nm and mean diameters of 40 ± 5 nm (Figs. 1d and 1e). Normalized standard deviation values (a standard deviation divided by a mean) in nanoneedle diameter and length distributions are as small as 0.16 and 0.06, respectively. These values are comparable to those of ZnO nanorods grown on Al₂O₃(0001) substrates and are one or two orders of magnitude smaller than those prepared by the catalyst-assisted VLS deposition method.^[6,8,14]

The size of the nanoneedles is controlled simply by changing the growth time, although it is also affected by other growth parameters such as temperature and pressure. From field-emission scanning electron microscopy (FE-SEM) images of ZnO nanoneedles grown at various growth times of 5, 10, and 60 min with fixed growth conditions, ZnO nanoneedles exhibited mean diameters of 13.2 ± 1.6 nm, 17.1 ± 2.6 nm, and 42.6 ± 6.9 nm and lengths of 79.1 ± 6.4 nm, 122.6 ± 6.8 nm, and 736.0 ± 44.9 nm, respectively, indicating increases in both their diameters and lengths over growth time. This result also shows that the rate of growth of the diameter is less than that of the length, which strongly suggests that nanoneedle formation originates from a higher growth rate along the *c*-axis direction than that along the in-plane direction. In order to confirm this argument, nanocrystal structure with less than 3 min growth time was investigated using synchrotron radiation X-ray diffraction (XRD). It showed a preferred *c*-axis orientation, and crystal orientation was unchanged during subsequent growth even though the shape changed.

The ZnO nanoneedles exhibited a preferred orientation along their *c*-axis. As shown in Figure 2, XRD θ - 2θ scan data show dominant peaks at 34.4° and 72.6° corresponding to ZnO(0002) and (0004) planes, respectively. This result indicates that nanoneedles exhibit their *c*-axes normal to the substrate surface. Meanwhile, the full width at half maximum (FWHM) values of XRD θ -rocking curves were 3 – 10° , which is an order of magnitude larger than those grown on Al₂O₃(0001) substrates.^[8] Additionally, ZnO nanoneedles grown on Si substrates showed random alignment along the in-plane direction, as determined by XRD ϕ -scan measurements. Similar results have been commonly observed in epi-

[*] Prof. G.-C. Yi, W. I. Park
Department of Materials Science and Engineering
Pohang University of Science and Technology (POSTECH)
Pohang, Kyungbuk 790-784 (Korea)
E-mail: gcyi@postech.ac.kr

Dr. M. Kim
Samsung Advanced Institute of Science and Technology
P. O. Box 111, Suwon 440-600 (Korea)

Dr. S. J. Pennycook
Oak Ridge National Laboratory
P. O. Box 2008, Oak Ridge 37831-6030 (USA)

[**] This work was supported by the POSTECH BSRI and CRM-KOSEF research funds. Extensive use of the facilities at POSTECH is acknowledged.

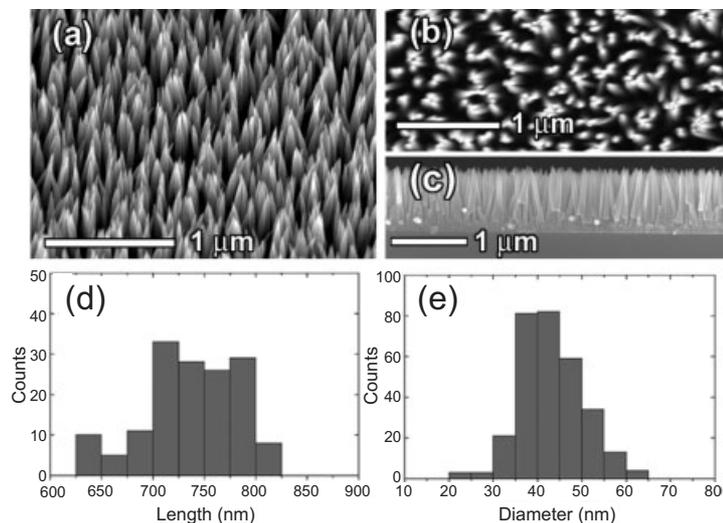


Fig. 1. FE-SEM images (tilted view (a), plan view (b), and cross-sectional view (c)) of ZnO nanoneedles and histograms of nanoneedle diameter (d) and length (e). a–c) Electron-microscopic images reveal that ZnO nanoneedles are in high density vertically aligned over the entire substrate and exhibit sharp tips. d,e) Nanoneedles grown for 1 h exhibit mean diameters and lengths of 40 ± 5 nm, 740 ± 50 nm, respectively.

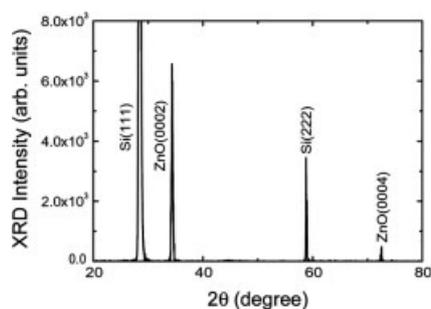


Fig. 2. XRD θ - 2θ scan data of ZnO nanoneedles on Si(111). XRD θ - 2θ scan data exhibit dominant peaks at 34.4° and 72.6° corresponding to ZnO(0002) and (0004) planes. This result indicates that nanoneedles exhibit their c -axes normal to the substrate surface.

taxial films, and are explained in terms of poor lattice mismatches and the possible formation of amorphous thin layers between ZnO and Si.^[15]

Transmission electron microscopy (TEM) was employed for further investigation of structural characteristics. In Figures 3a and 3b, low-magnification TEM images show the general morphology of individual nanoneedles. While the lower parts of the ZnO nanoneedles show uniform diameters along the nanoneedle stems, their tips exhibit the extreme sharp morphology. The interior angle of the tips ranged from 12° to 25° . No metal clusters were observed on the nanoneedle tips, in contrast to nanoneedles grown by the catalysis-assisted VLS method.^[1,6] In addition, the absence of metal impurities was confirmed by energy-dispersive X-ray spectroscopy (EDX) in the detection limit, indicating that the nanoneedles were grown by a non-catalytic growth mechanism.

Figures 3c and 3d show high-resolution scanning TEM (STEM) images of ZnO nanoneedles measured along the stems. In the high-angle annular dark-field image (d), a so-called Z-contrast image, we can see the zigzag of Zn atoms in a hexagonal unit cell and this atomic configuration continues to the edge of the surface. In addition, dislocations and stacking faults were rarely observed. These results indicate that individual ZnO nanoneedles are practically defect-free single

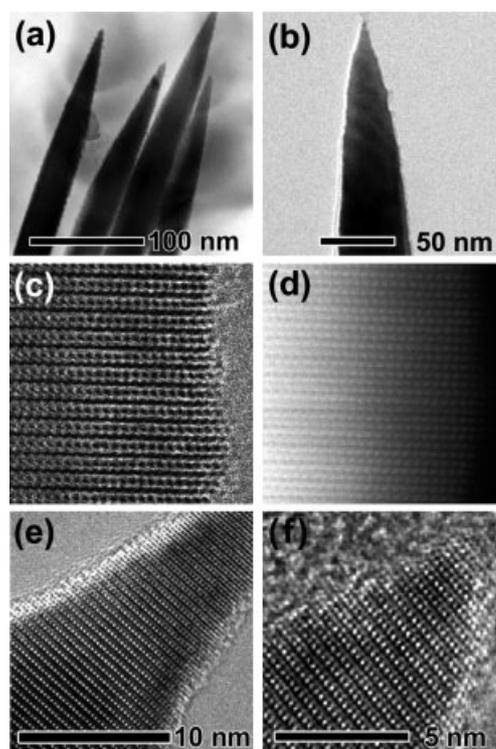


Fig. 3. TEM images of ZnO nanoneedles. a,b) Low-magnification TEM images show extremely sharp morphology of the nanoneedle tips. c,d) High-resolution STEM images exhibit lattice fringes clearly observed in both bright field images (c) and annular dark field Z-contrast images (d). The lattice spacing between adjacent lattice planes corresponds to the d -spacing of (0001) planes and is 0.26 nm. e,f) High-resolution TEM images of the tips also show clear lattice images without any significant defects.

crystals. The lattice spacing between adjacent lattice planes corresponds to the d -spacing of the (0001) planes and is 0.26 nm. From the TEM images of all of the nanoneedles investigated in this study, only the (000 l) planes are perpendicular to the growth direction of nanoneedles, indicating that ZnO nanoneedles only grow along the [0001] direction. High-resolution TEM images measured along the ZnO nanoneedle tips also show the highly ordered lattice images in Figures 3e

and 3f. The nanoneedles, as shown in Figure 3e, gradually taper down from several tens of nanometers and so exhibit only a few atoms on their tips as shown in Figure 3f. Hence, the typical curvature radii measured at the tip apexes are 1 or 2 nm.

The optical properties of the ZnO nanoneedles were investigated by photoluminescence (PL) spectroscopy. Figure 4 shows a room-temperature PL spectrum of ZnO nanoneedles. A dominant near-band-edge emission peak was observed at

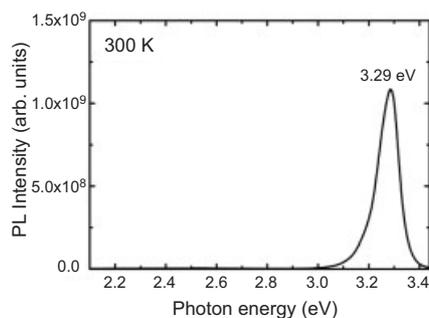


Fig. 4. PL spectrum of ZnO nanoneedles measured at room temperature. The PL spectrum shows a dominant near-band-edge emission peak at 3.29 eV with a very weak deep-level emission band.

3.29 eV, which is attributed to a free exciton peak.^[10,15,16] The FWHM value of this excitonic emission peak is 90 meV, which is comparable to that of ZnO epilayers.^[10,15,16] It is also noted that the PL peak position shows no blueshift in band-edge emission.^[6,8,13]

ZnO nanoneedles exhibited a very weak deep-level emission band compared with the free excitonic emission. The origin of the deep level in ZnO is not yet clearly understood but is generally attributed to structural defects, single ionized vacancies, and impurities.^[6,13] Since our ZnO nanoneedles are grown at a low temperature by direct atomic adsorption without mediation of any foreign elemental catalyst, unintentional incorporation of metal impurities into nanoneedles can be avoided. In addition, as determined from the TEM study, individual ZnO nanoneedles are almost defect-free and are single-crystals. Accordingly, the excellent optical properties, evident in strong excitonic emission peaks with a weak deep-level emission band, could be attributed to the high purity and crystallinity of the ZnO nanoneedles. In addition to the excellent optical properties of the catalyst-free MOCVD-grown ZnO nanoneedles, reduction in impurity incorporation and defect formation make it easy to precisely control the conductivity in a wide range, essential for many device applications. Hence, a catalyst-free method of growing nanoneedles with low defect concentrations yields ideal building blocks for high-performance device fabrications.

In conclusion, ZnO nanoneedles were grown vertically on Si substrates using MOCVD without employing any metal catalysts as usually required with other methods. Electron microscopy revealed that nanoneedles with sharp tips were grown vertically from substrates with uniform distributions in their diameters, lengths, and densities. Furthermore, these

nanoneedles have high crystallinity and excellent photoluminescent characteristics. From the PL spectra measured at room temperature, a narrow and strong emission peak was observed at 3.29 eV with a very weak deep-level emission, indicating that the nanoneedles are of high optical quality.

Experimental

ZnO nanoneedles were grown on Si(111) substrates using a low-pressure MOCVD system. Diethyl zinc (Et_2Zn) and oxygen were the reactants and their flow rates were in the range of 20–100 sccm and 0.5–5 sccm, respectively. Typical growth temperatures were in the 400–500 °C range. Prior to nanoneedle growth, the substrates were cleaned in an ultrasonic bath with acetone and methanol. During the nanoneedle growth, no metal catalyst was coated on the substrates.

High-resolution TEM analysis was performed using Philips Tecnai UT-30, and High-resolution STEM analysis with a VG Microscopes HB603U. The TEM nanoneedle specimens were prepared by scratching the as-grown sample surface, dispersing the pieces in alcohol, then depositing them on a carbon-coated copper grid. Although neither ultrasonication nor surfactant was used for the separation of individual nanoneedles, they are well-isolated.

PL spectroscopy was employed for optical characterization of the nanoneedles. The PL measurements were performed at room temperature with an optical resolution of 0.02–0.1 nm, and the 325 nm line of a continuous-wave He–Cd laser was used as the excitation source. Details of the PL measurements have been reported previously [16]. The PL measurements were performed at 10–300 K using a Displex refrigeration system.

Received: July 22, 2002
Final version: September 26, 2002

- [1] J. D. Holmes, K. P. Johnston, R. C. Doty, B. A. Korgel, *Science* **2000**, 287, 1471.
- [2] Z. W. Pan, Z. R. Dai, Z. L. Wang, *Science* **2001**, 291, 1947.
- [3] W. Han, S. Fan, Q. Li, Y. Hu, *Science* **1997**, 277, 1287.
- [4] W. A. de Heer, A. Châtelain, D. Ugarte, *Science* **1995**, 270, 1179.
- [5] P. Kim, C. M. Lieber, *Science* **1999**, 286, 2148.
- [6] a) M. H. Huang, Y. Wu, H. Feick, N. Tran, E. Weber, P. Yang, *Adv. Mater.* **2001**, 13, 113. b) M. H. Huang, S. Mao, H. Feick, H. Yan, Y. Wu, H. Kind, E. Weber, R. Russo, P. Yang, *Science* **2001**, 292, 1897.
- [7] R. S. Wagner, W. C. Ellis, *Appl. Phys. Lett.* **1964**, 4, 89.
- [8] W. I. Park, D. H. Kim, S.-W. Jung, G.-C. Yi, *Appl. Phys. Lett.* **2002**, 80, 4232.
- [9] D. G. Thomas, *J. Phys. Chem. Solids* **1960**, 15, 86.
- [10] D. M. Bagnall, Y. F. Chen, Z. Zhu, T. Yao, M. Y. Shen, T. Goto, *Appl. Phys. Lett.* **1998**, 73, 1038.
- [11] Z. K. Yang, P. Yu, G. K. L. Wong, M. Kawasaki, A. Ohtomo, H. Koinuma, Y. Segawa, *Solid State Commun.* **1997**, 103, 459.
- [12] W. I. Park, G.-C. Yi, H. M. Jang, *Appl. Phys. Lett.* **2001**, 79, 2022.
- [13] J.-J. Wu, S.-C. Liu, *Adv. Mater.* **2002**, 14, 215.
- [14] M. S. Gudiksen, C. M. Lieber, *J. Am. Chem. Soc.* **2000**, 122, 8801.
- [15] W. I. Park, G.-C. Yi, *J. Electron. Mater.* **2001**, 30, L32.
- [16] S. W. Jung, W. I. Park, H. D. Cheong, G.-C. Yi, H. M. Jang, S. Hong, T. Joo, *Appl. Phys. Lett.* **2002**, 80, 1924.